Results of the Department of Space Physics, Institute of Atmospheric Physics, Czech Academy of Sciences, published in 2015

1. Whistler mode chorus and hiss

The Time History of Events and Macroscale Interactions during Substorms (THEMIS)-D spacecraft crossed an active equatorial source region of whistler mode chorus rising tones on 23 October 2008. We analyzed the chorus rising tones in terms of spectral and polarization characteristics, with special emphasis on wave normal angles. The latter exhibited large variations from quasi-parallel to oblique, even within single bursts, but seemed to follow a definite pattern, which enabled an unambiguous classification into five different groups. We also discussed the frequently observed splitting of chorus bursts into a lower and an upper band around one half of the local electron cyclotron frequency. At chorus frequencies close to the gap, we found significantly lowered wave planarities and a tendency of wave normal angles to approach the Gendrin angle.

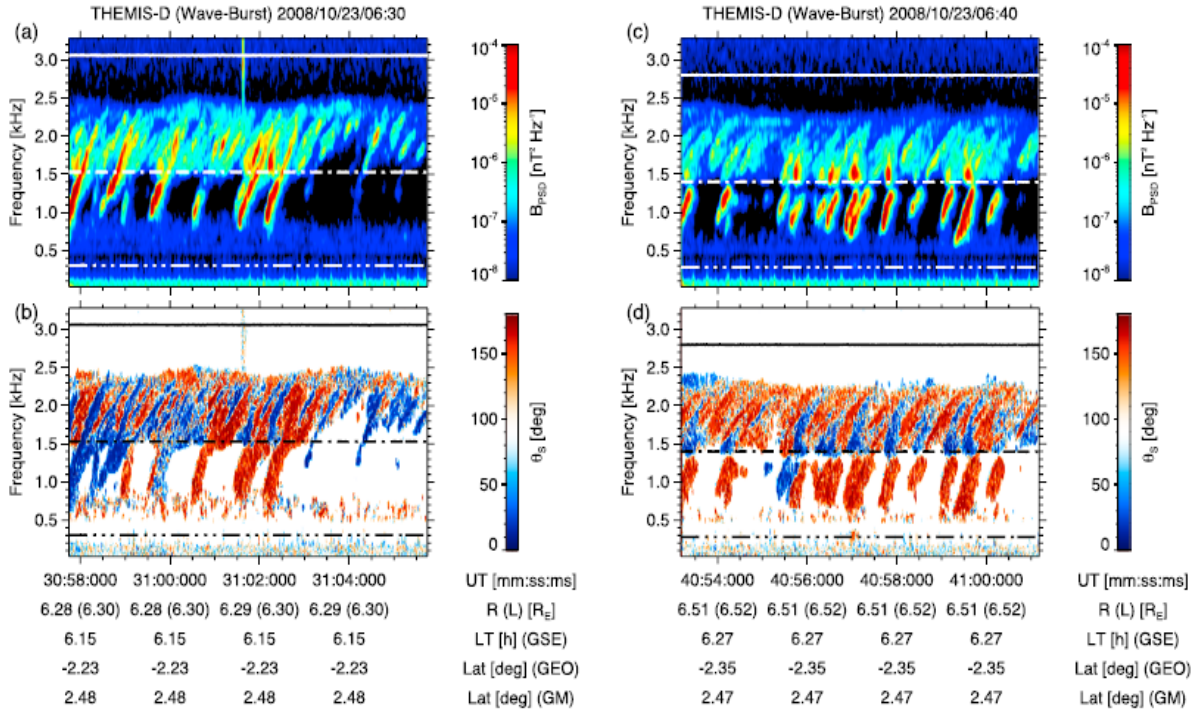

(a, c) Magnetic power spectral density and (b, d) polar angle of the Poynting vector for two THEMIS-D wave burst snapshots from 23 October 2008. The local electron cyclotron frequency f_{ce} as well as 0.5 f_{ce} and 0.1 f_{ce} are indicated by solid, dash-dotted, and dash-dot-dot-dot lines.

Reference:

Taubenschuss U., Santolík O., Graham D. B., Fu H., Khotyaintsev Y. V., Le Contel O., 2015: Different types of whistler mode chorus in the equatorial source region. Geophys. Res. Lett., 42, doi:10.1002/2015GL066004.

Related references:

Macúšová, E., O. Santolík, N. Cornilleau-Wehrlin, and K. H. Yearby (2015), Bandwidths and amplitudes of chorus-like banded emissions measured by the TC-1 Double Star spacecraft, J. Geophys. Res. Space Physics, 120, 1057-1071, doi:10.1002/2014JA020440.

Miyoshi, Y., S. Saito, K. Seki, T. Nishiyama, R. Kataoka, K. Asamura, Y. Katoh, Y. Ebihara, T. Sakanoi, M, Hirahara, S. Oyama, S. Kurita, and **O. Santolík** (2015), Relation between fine structure of energy spectra for pulsating aurora electrons and frequency spectra of whistler mode chorus waves, J. Geophys. Res. Space Physics, 120, doi:10.1002/2015JA021562.

Miyoshi, Y., S. Oyama, S. Saito, S. Kurita, H. Fujiwara, R. Kataoka, Y. Ebihara, C. Kletzing, G. Reeves**, O. Santolík**, M. Clilverd, C. J. Rodger, E. Turunen, and F. Tsuchiya (2015), Energetic electron precipitation associated with pulsating aurora: EISCAT and Van Allen Probe observations, J. Geophys. Res. Space Physics, 120, 2754–2766, doi:10.1002/2014JA020690.

Hajra, R., B. T. Tsurutani, E. Echer, W. D. Gonzalez, C. G. Marques Brum, L. E. Antunes Vieira, and **O. Santolík** (2015), Relativistic Electron Acceleration during HILDCAA Events: Are Precursor CIR Magnetic Storms Important? Earth, Planets and Space 67:109, DOI 10.1186/s40623-015-0280-5.

Laakso, H., **O. Santolík**, R. Horne, **I. Kolmašová**, P. Escoubet, A. Masson, and M. Taylor (2015), Identifying the source region of plasmaspheric hiss, Geophys. Res. Lett., 42, 3141-3149, doi:10.1002/2015GL063755.

Tsurutani, B. T., B. J. Falkowski, J. S. Pickett, **O. Santolík**, and G. S. Lakhina (2015), Plasmaspheric hiss properties: Observations from Polar, J. Geophys. Res. Space Physics, 120, 414-431, doi:10.1002/2014JA020518.

Titova, E. E., B. V. Kozelov, A. G. Demekhov, J. Manninen, **O. Santolík**, C. A. Kletzing, and G. Reeves (2015), Identification of the source of quasiperiodic VLF emissions using ground-based and Van Allen Probes satellite observations, Geophys. Res. Lett., 42, 6137–6145, doi:10.1002/2015GL064911.

2. Equatorial noise

We reported results of a systematic analysis of whistler-mode equatorial noise (EN) emissions which are also known as fast magnetosonic waves. EN occurs in the vicinity of the geomagnetic equator at frequencies between the local proton cyclotron frequency and the lower hybrid frequency. Our analysis was based on the data collected by the Spatio-Temporal Analysis of Field Fluctuations–Spectrum Analyzer (STAFF-SA) instruments on board the four Cluster spacecraft. The analyzed data set covered the period from January 2001 to December 2010. We developed selection criteria for the visual identification of these emissions, and we compiled a list of more than 2000 identified events. The evolution of the Cluster orbit enabled us to investigate a large range of McIlwain's parameter from about L∼1.1 to L∼10. We demonstrated that EN can occur at almost all analyzed L shells. However, the occurrence rate was very low (<6%) at L shells below L=2.5 and above L=8.5. EN mostly occurred between L=3 and L=5.5, and within 7◦ of the geomagnetic equator, reaching 40% occurrence rate. This rate further increased to more than 60% under geomagnetically disturbed conditions. Analysis of occurrence rates as a function of magnetic local time (MLT) showed strong variations outside of the

plasmasphere (with a peak around 15 MLT), while the occurrence rate inside the plasmasphere was almost independent on MLT. This is consistent with the hypothesis that EN is generated in the afternoon sector of the plasmapause region and propagates both inward and outward.

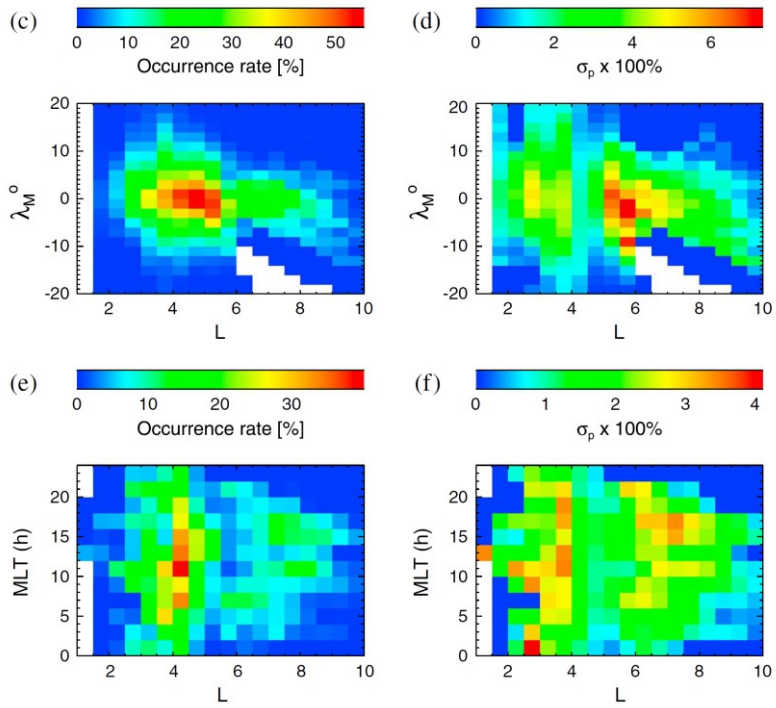

Occurrence rates of equatorial noise and their estimated standard deviations in the bins 0.5 L × 2°λ_M (c, e) and 0.5 L × 2 h MLT (d, f), respectively.

Reference:

Hrbáčková, Z., O. Santolík, F. Nemec, **E. Macúšová**, and N. Cornilleau-Wehrlin (2015), Systematic analysis of occurrence of equatorial noise emissions using 10 years of data from the Cluster mission, J. Geophys. Res. Space Physics, 120, 1007-1021, doi:10.1002/2014JA020268.

Related references:

Balikhin, M. A., Y. Y. Shprits, S. N. Walker, L. Chen, N. Cornilleau-Wehrlin, I. Dandouras, **O. Santolik**, C. Carr, K. H. Yearby, B. Weiss, Observations of discrete harmonics emerging from equatorial noise (2015). Nat. Commun. 6:7703 doi: 10.1038/ncomms8703.

Němec, F., **O. Santolík, Z. Hrbáčková**, J. S. Pickett, and N. Cornilleau-Wehrlin (2015), Equatorial noise emissions with quasiperiodic modulation of wave intensity, J. Geophys. Res. Space Physics, 120, 2649-2661, doi:10.1002/2014JA020816.

Němec, F., **O. Santolík, Z. Hrbáčková**, and N. Cornilleau-Wehrlin (2015), Intensities and spatiotemporal variability of equatorial noise emissions observed by the Cluster spacecraft, J. Geophys. Res. Space Physics, 120, 1620-1632, doi:10.1002/2014JA020814.

3. Wave emissions observed by the low-altitude satellite DEMETER

We presented an analysis of ULF (0–20 Hz) waves observed by the low-altitude satellite Detection of Electro-Magnetic Emissions Transmitted from Earthquake Regions (DEMETER) during the magnetic storm of November 2004. Since these ULF waves were measured by both electric and magnetic antennas, we were able to identify them as electromagnetic ion cyclotron (EMIC) waves. This is the first time that they were observed for such extensive time periods and at such high frequencies. The analysis of wave propagation pointed to the possible source region placed in the inner magnetosphere (L~2–3). Observed wave frequencies indicated that waves were generated much farther from the Earth compared to the satellite orbit. Exceptionally high frequencies of about 10 Hz were explained by the source region placed in the deep inner magnetosphere at L ~2.5. We hypothesized that these waves were generated below the local helium gyrofrequency and propagated over a large range of wave normal angles to reach low altitudes at L~1.11.

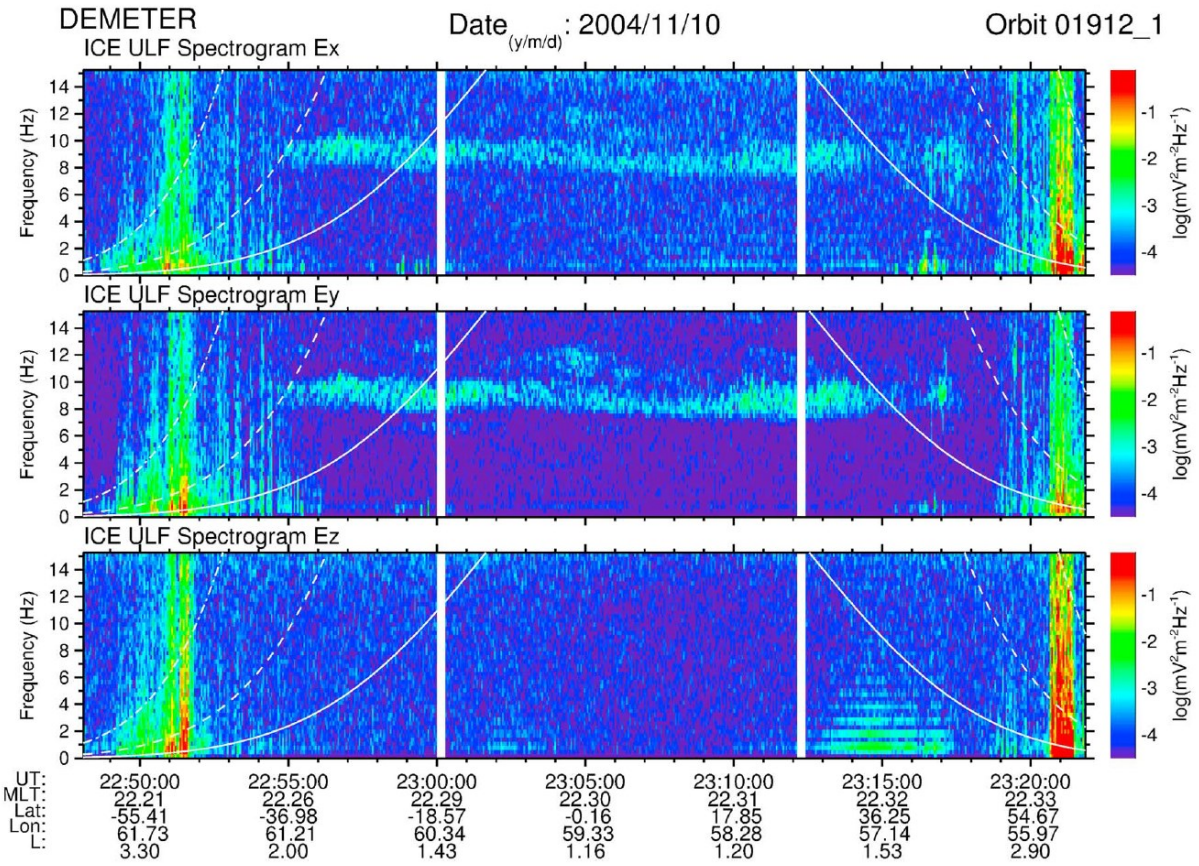

ULF spectrograms of the three electric components up to 15 Hz. The data are recorded on 10 November 2004 between 22:48:06 and 23:21:44 UT. The parameters below are the universal time (UT), the magnetic local time (MLT), the geomagnetic latitude and longitude, and McIlwain parameter (L). The vertical white lines indicate data gaps due to calibration. The solid, dashed, and dash-dotted white lines indicate equatorial O+, He+, and H+ cyclotron frequencies traced from the satellite position.

Reference:

Píša, D., M. Parrot, **O. Santolík**, and J. D. Menietti (2015), EMIC waves observed by the low-altitude satellite DEMETER during the November 2004 magnetic storm, J. Geophys. Res. Space Physics, 120, 5455-5464, doi:10.1002/2014JA020233.

Related references:

Bezděková, B., F. Němec, M. Parrot, **O. Santolík**, and **O. Krupařová** (2015), Magnetospheric line radiation: 6.5 years of observations by the DEMETER spacecraft, J. Geophys. Res. Space Physics, 120, 9442–9456, doi:10.1002/2015JA021246.

Nemec, F., M. Parrot, and **O. Santolík** (2015), Power line harmonic radiation observed by the DEMETER spacecraft at 50/60 Hz and low harmonics, J. Geophys. Res. Space Physics, 120, 8954-8967, doi:10.1002/2015JA021682.

4. Electromagnetic manifestation of lightning activity

Both unipolar and bipolar magnetic or electric field pulses were observed during preparatory stages of a lightning flash. We introduced a new simple analytical model to describe both kinds of pulses. We showed how the polarity overshoot depended on the parameters of the model, including the propagation velocity of the current pulse, the step length, and the injected current waveshape. We observed that the expression for the radiation part of the magnetic field decomposed into two time-shifted terms with opposite polarities. The model well corresponded not only to observations of the bipolar preliminary breakdown pulses at time scales of tens of microseconds but also to both unipolar and bipolar dart-stepped leader pulses at submicrosecond time scales.

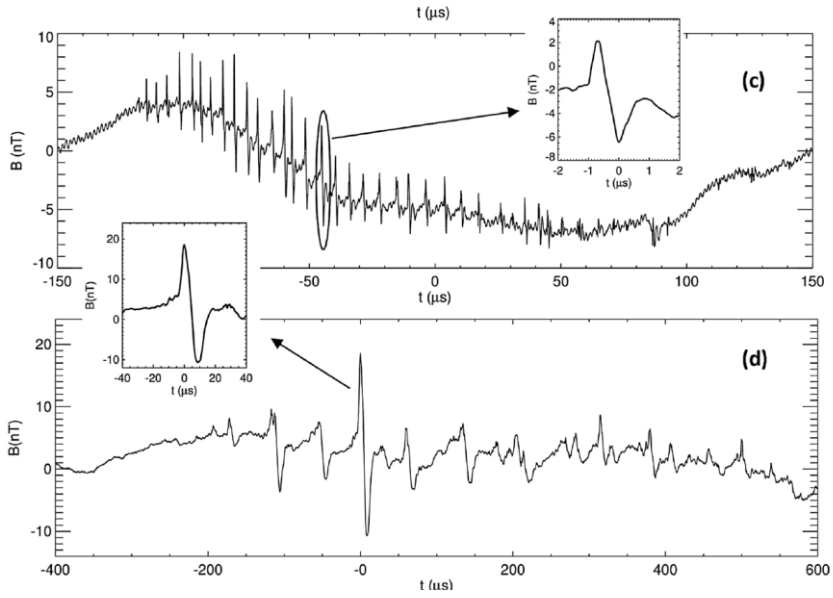

(c) Example of a sequence composed from bipolar pulses. (d) Example of a sequence of bipolar pulses preceding the first negative cloud-to-ground lightning discharge. Detailed examples of individual pulses are shown in the insets.

Reference:

Kašpar, P., **O. Santolík**, and **I. Kolmašová** (2015), Unipolar and bipolar pulses emitted during the development of lightning flashes, Geophys. Res. Lett., 42, 7206-7213, doi:10.1002/2015GL064777.

Related references:

Záhlava, J., F. Nemec, **O. Santolík**, **I. Kolmašová**, M. Parrot, and C. J. Rodger (2015), Very low frequency radio events with a reduced intensity observed by the low-altitude DEMETER spacecraft, J. Geophys. Res. Space Physics, 120, 9781-9794, doi:10.1002/2015JA021607.

Parrot, M., J. J. Berthelier, J. Blecki, J. Y. Brochot, Y. Hobara, D. Lagoutte, J. P. Lebreton, F. Nemec, T. Onishi, J. L. Pinçon, **D. Píša**, **O. Santolík**, J. A. Sauvaud, E. Slominska (2015), Unexpected events recorded by the ionospheric satellite DEMETER, Surveys in Geophysics 36(3), 483-511.

5. Solar wind and magnetospheric boundaries

We presented results of a statistical study of the distribution of mirror and Alfvén-ion cyclotron (AIC) waves in the magnetosheath together with plasma parameters important for the stability of ULF waves, specifically ion temperature anisotropy and ion beta.

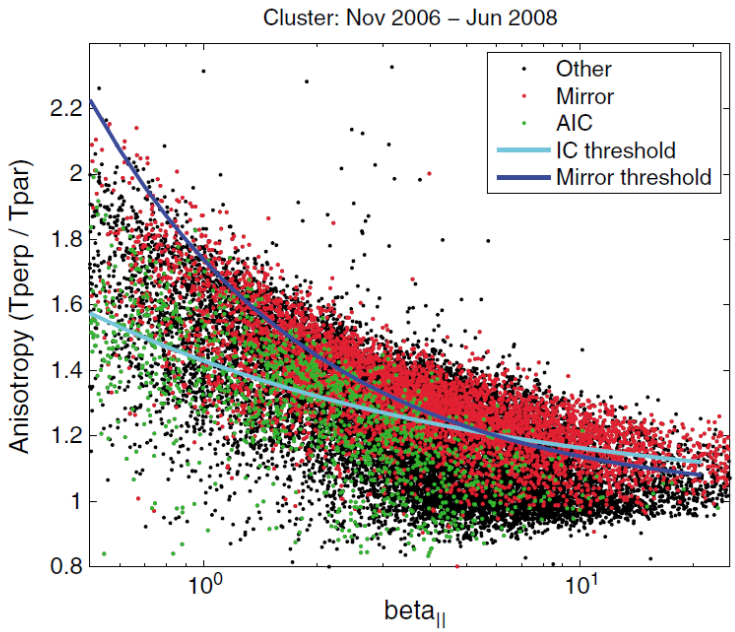

Distribution of observed wave types in the anisotropy-β∥ space. Red dots indicate intervals with identified mirror modes, green dots with AIC waves, and black dots the remaining intervals in the statistical data set. Overplotted are the instability thresholds for mirror and ion cyclotron instabilities.

Magnetosheath crossings registered by Cluster spacecraft over the course of 2 years served as a basis for the statistics. For each observation we used bow shock, magnetopause, and magnetosheath flow models to identify the relative position of the spacecraft with respect to magnetosheath boundaries and

local properties of the upstream shock crossing. A strong dependence of both plasma parameters and mirror/AIC wave occurrence on upstream Θ_{Bn} and M_A was identified. We analyzed a joint dependence of the same parameters on Θ_{Bn} and fractional distance between shock and magnetopause, zenith angle, and length of the flow line. Finally, the occurrence of mirror and AIC modes was compared against the respective instability thresholds. We noted that AIC waves occurred nearly exclusively under mirror stable conditions. This was interpreted in terms of different characters of nonlinear saturation of the two modes.

Reference:

Souček J., Escoubet C. P., **Grison B**., 2015: Magnetosheath plasma stability and ULF wave occurrence as a function of location in the magnetosheath and upstream bow shock parameters. J. Geophys. Res. Space Physics, 120, 2838–2850, doi:10.1002/2015JA021087.

Related references:

Krupař, V., E. P. Kontar, **J. Soucek**, **O. Santolik**, M. Maksimovic, and **O. Krupařová** (2015), On the speed and acceleration of electron beams triggering interplanetary type III radio bursts, Astronomy & Astrophysics 580, A137, doi: 10.1051/0004-6361/201425308.

Krupařová, O., L. Přech, K. Jelínek, Š. Dusik, J. Šimůnek, K. Grygorov, and J.-H. Shue (2015), Analysis of temperature versus density plots and their relation to the LLBL formation under southward and northward IMF orientations, J. Geophys. Res. Space Physics, 120, 3475–3488, doi:10.1002/2014JA020308.

Krupařová, O., J. Šafránková, Z.Němeček, and L. Přech (2015), Transient events at the magnetopause and bipolar magnetic signatures, Planetary and Space Science 115, 9–26.

6. Statistics of Langmuir wave amplitudes observed inside Saturn's foreshock by the Cassini spacecraft

We presented the first systematic study of Langmuir wave amplitudes in Saturn's foreshock using the Cassini Radio and Plasma Wave Science/Wideband Receiver measurements. We analyzed all foreshock crossings from June 2004 to December 2009 using an automatic method to identify Langmuir waves. Using this method, almost 3×10^5 waveform intervals of typical duration of about a minute were selected. For each selected waveform interval, the position of the satellite inside the foreshock was calculated using an adaptive bow shock model, which was parametrized by the observed magnetic field and plasma data. We determined the wave amplitudes for all waveform intervals, and we found that the probability density function amplitudes follow a lognormal distribution with a power law tail. A nonlinear fit for this tail gave us a power law exponent of -1.37 ± 0.01. The distribution of amplitudes as a function of the depth in the foreshock showed the onset of the waves near the upstream boundary with its maximum slightly shifted inside the foreshock ($\sim$1 RS). The amplitudes then fell off with increasing depth in the downstream region. Our results were in agreement with previous observations and roughly followed the generally accepted stochastic growth theory mechanism for the foreshock region, with an exception at the highest observed amplitudes. The estimated energy density ratio W for largest amplitudes did not exceed 10^{-2}, suggesting that modulational instability was not relevant for a

large majority of waves. The decay instability can be important for the stronger electrostatic waves in Saturn's foreshock, as was previously reported for multiple solar system planets.

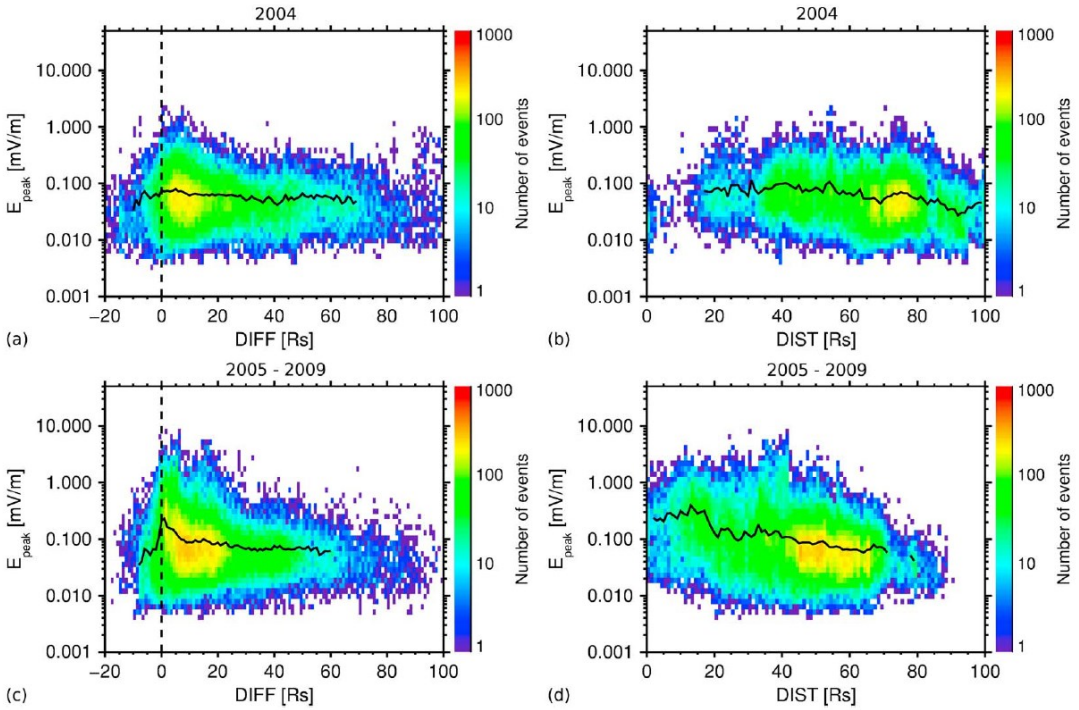

Number of waveform intervals in equidistant bins 0.1 log(mV/m) × 1 RS as a function of the logarithm of the wave amplitude and (a, c) the depth (DIFF) inside the foreshock and (b, d) the distance from the tangent point along the magnetic field tangent line (DIST). The vertical dashed black line shows the upstream boundary of the bow shock (DIFF = 0). Median of the wave amplitude over foreshock coordinates is plotted by the black line with a 1 RS step for positions with more than 100 points.

Reference:

Píša, D., G. B. Hospodarsky, W. S. Kurth, **O. Santolík**, **J. Souček**, D. A. Gurnett, A. Masters, and M. E. Hill (2015), Statistics of Langmuir wave amplitudes observed inside Saturn 's foreshock by the Cassini spacecraft, J. Geophys. Res. Space Physics, 120, 2531-2542, doi:10.1002/2014JA020560.

Department of Space Physics, Institute of Atmospheric Physics of the Czech Academy of Sciences in 2015

1. Marek Basovník, PhD student, 60% FTE
2. Benjamin Grison, research scientist
3. Michajlo Hajoš, research scientist
4. Miroslav Horký, postdoctoral associate, since November 1
5. Zuzana Hrbáčková, PhD student, 70% FTE
6. Petr Kašpar, postdoctoral associate
7. Vratislav Krupař, postdoctoral associate, until August 31; 20% FTE since September 1
8. Oksana Krupařová, postdoctoral associate
9. Eva Macúšová, postdoctoral associate
10. Radek Lán, research engineer
11. David Píša, postdoctoral associate
12. Ondřej Santolík, senior research scientist, head of the department
13. Jan Souček, research scientist, deputy head of the department
14. Ulrich Taubenschuss, research scientist
15. Alexander Tomori, PhD student, 50% FTE
16. Hana Zemanová, PhD student, 40% FTE since November 1